IRSTI 28.23.15 https://doi.org/10.26577/jpcsit4220263

Zaki Al-Farabi, Ilyas Umurbekov, Iliyas Tursynbek, Adilet Yesbayev, Zhanibek Rysbek, Almaskhan Baimyshev, Zhanat Kappassov*

Nazarbayev University, Astana, Kazakhstan
*e-mail: zhkappassov@nu.edu.kz

LOW-COST NIGHT VISION CAMERA BASED ON A MODIFIED CONSUMER WEBCAM AND LIGHTWEIGHT REAL-TIME ENHANCEMENT

Abstract. Low-light perception is a core requirement for robotics, inspection, and wearable situational awareness, yet reliable night- vision solutions often require expensive sensors or computationally heavy processing. This manuscript presents (i) a low-cost near- infrared (NIR) night-vision camera system with real-time enhancement and mixed-reality visualization, and (ii) a controlled benchmarking protocol that compares multiple sensor modalities and classical en- hancement pipelines on a Linux embedded platform. To prioritize real-time feasibility, we deliberately avoid neural networks and other AI/ML models, and instead benchmark lightweight classical methods: CLAHE, bilateral filtering + CLAHE, Non-Local Means (NLM) + CLAHE, Retinex SSR, Retinex SSR with percentile normalization, and two proposed pipelines (a CLAHE-based pipeline and a Retinex integrated variant). Experiments were conducted in a fully dark room using identical illumination conditions and multiple observation distances. We report runtime (ms/frame, FPS) and no- reference quality metrics (entropy, edge strength, Laplacian variance, RMS contrast, mean intensity) to accommodate the absence of ground-truth references. A representative run shows that the proposed CLAHE-based pipeline achieves 246.5 FPS at 640×480 while substantially improving objective no-reference metrics relative to raw frames, whereas Retinex with percentile normalization yields higher contrast/entropy but at 12.7 FPS. Hardware benchmarking indicates that thermal imaging provides the clearest visibility but at high cost/power, Kinect requires stronger illumination, and event-based sensing offers extremely low latency but requires temporal modulation to observe static targets.

Keywords: night vision, low-light enhancement, Retinex, CLAHE, embedded vision, Jetson, event camera, thermal camera, HoloLens.

1. Introduction

Night-vision sensing enables perception in environments where visible-light cameras fail, including nighttime naviga- tion, surveillance, search-and-rescue, and industrial inspection. Low-light frames commonly exhibit reduced contrast and amplified noise due to sensor gain and exposure control, motivating enhancement methods that improve visibility while preserving structure [1], [2].

Classical enhancement pipelines remain attractive for embedded systems because they are transparent, lightweight, and do not require training data or model deployment. Local contrast enhancement is often performed using adaptive histogram equalization and its variants [3], including contrast-limited adaptive histogram equalization (CLAHE) [4], [5]. Edge- preserving smoothing can be performed using anisotropic diffusion [6] or bilateral filtering [7], while patch-based denoising such as Non-Local Means can yield strong noise suppression at higher computational cost [8]. Illumination normalization is frequently addressed with Retinex theory [9] and practical center/surround Retinex formulations [10]. These classical methods contrast with learning-based low-light enhancement approaches such as LIME [11], RetinexNet [12], and Zero- DCE [13], which can provide strong enhancement but typically increase system complexity and may exceed the intended compute budget for lightweight embedded deployment.

This manuscript benchmarks both hardware and software under identical dark-room conditions. Hardware includes a thermal camera (FLIR T540 class) [14], Xbox Kinect v1 [15], an event-based camera platform (Prophesee Metavision EVK4-HD class) [16]–[18], and our own low-cost NIR camera system. Software benchmarking compares multiple classical pipelines in real time and reports metrics to support objective comparison imagery. The complete system source code is available publicly [19]. An overview of the real-time enhancement pipeline and MJPEG streaming workflow is shown in Figure 1.

Figure 1
Overview of the real-time enhancement pipeline and MJPEG streaming to HoloLens

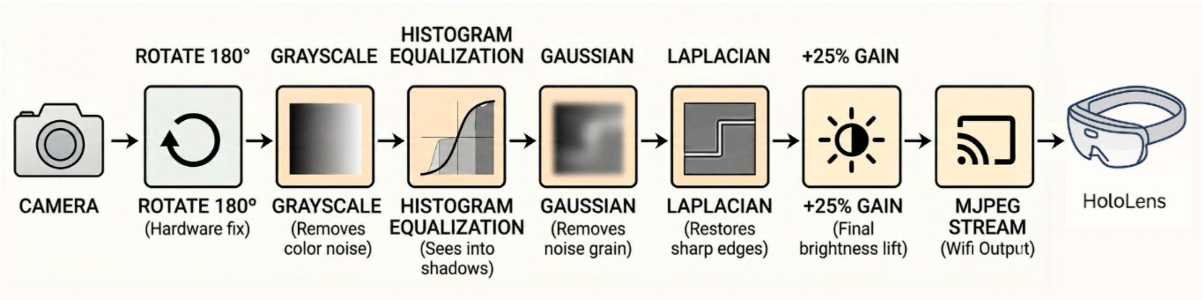

2. Materials and methods

2.1 Embedded Platform and System Implementation

All experiments were executed on an NVIDIA Jetson Orin NX (16GB-class) embedded platform running Linux [20]. The capture-process-record pipeline was implemented in C++ using OpenCV [21], which enables native compilation and access to optimized image processing primitives commonly used in real-time vision systems. The proposed system is designed for low-latency streaming: enhanced frames are encoded and streamed as MJPEG to multiple clients for visualization, including a Unity-based client running on HoloLens 2 [22].

2.2 3D Printed Enclosure

To house the modified camera and IR emitter as a compact unit, a custom enclosure was designed using CAD software and manufactured using a 3D printer. The enclosure provides structural stability, protects internal components, and ensures that the emitter and lens remain fixed and aligned during operation. The handle mounted on the enclosure facilitates handheld operation and improves device portability. Figure 2 shows the CAD rendering of the final enclosure used in the prototype.

Figure 2
CAD model of the camera enclosure with IR emitter

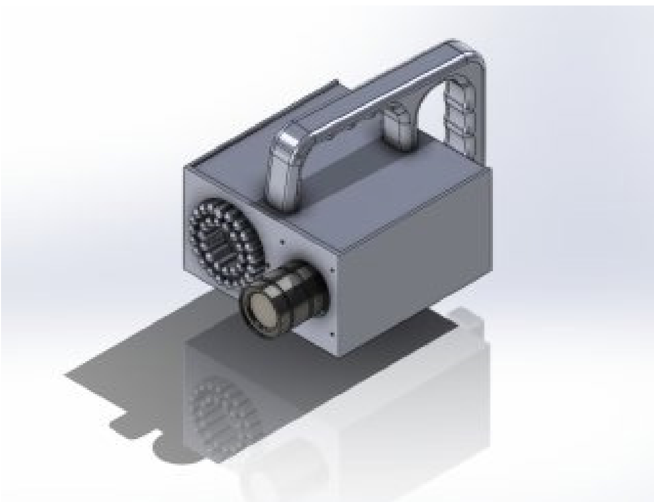

2.3 Controlled Dark-Room Recording Protocol

All experiments used the same scene: a blue box placed on a white table in a completely dark room without external illumination. For each camera type, we recorded 20-second videos at 50, 100, 150, and 250 cm observation distances. For the software benchmarking and Kinect trials, a person walked back and forth across the field of view to provide a qualitative temporal reference for motion smoothness and perceived latency.

Event-based sensors produce events primarily in response to temporal intensity changes [18]. Therefore, for a static scene we engineered a flickering IR illumination pattern (approximately 5 ms period) to induce controlled brightness changes and enable observation.

2.4 Hardware Benchmarking Cameras

We evaluated four sensing modalities:

1) Thermal camera: FLIR T540-class device, used as a high-quality reference for visibility in complete darkness [14].

2) Xbox Kinect v1: consumer depth/IR sensor family [15]. To keep comparisons focused on intensity-based night- vision, we do not include depth outputs in the primary image-quality comparison.

3) Event-based camera: Prophesee Metavision EVK4-HD family [16], leveraging event-based sensing principles [17], [18].

4) Our low-cost NIR camera: a consumer camera con- figured for NIR sensitivity, evaluated with the same illumination source as the Kinect and software tests.

2.5 Proposed Image Enhancement Pipeline

In our hardware VR setup, we developed a real-time "Grid Mode" visualization, as can be seen in Fig. 3. This debugging tool stitches the output of every intermediate processing step into a single 2 x 3 video matrix, allowing simultaneous comparison of effects of filters implemented in our pipeline. The following filters were implemented to provide the most effective results in this exact order:

1) Baseline (Grayscale Input): We observed that the raw input suffered from extremely low dynamic range. Details in shadowed areas were indistinguishable from the background.

2) CLAHE (Local Contrast): Application of CLAHE successfully recovered details in the dark regions. However, this step introduced a significant side effect: the amplification of sensor noise, resulting in visible "grain" or "salt-and-pepper" artifacts.

3) Gaussian Denoising: By applying a 3 x 3 Gaussian blur, we successfully suppressed the grain introduced by CLAHE. While this resulted in a cleaner image, it inevitably softened object boundaries, slightly reducing the sharpness.

4) Laplacian Sharpening: To counteract the smoothing from the denoising step, Laplacian filtering was applied. This restored the structural edges of obstacles without re-introducing the background noise, effectively "popping" objects from the background.

5) Linear Gain (Brightness Boost): Finally, a linear scaling factor of 1.25 (+25%) was applied. This ensured that the final image is brighter

This distinct separation of concerns, where one filter cor- rects the artifacts introduced by the previous one-proved superior to attempting to solve all issues with a single complex algorithm.

Figure 3

Demonstration of filters' effect

2.6 Software Benchmarking Pipelines

To target lightweight embedded deployment, this manuscript intentionally avoids neural networks and other AI/ML models. We benchmarked the following classical real-time pipelines at 640×480 resolution:

1. Raw grayscale (no enhancement).
2. CLAHE-only [4].
3. Bilateral + CLAHE [4], [7].
4. NLM + CLAHE [4], [8].
5. Retinex SSR grounded in Retinex theory [9] and center/surround Retinex enhancement [10].
6. Retinex SSR + percentile normalization (RetinexSSR_Pctl), using robust intensity scaling to reduce sensitivity to outliers (contrast scaling background [1]).
7. Proposed: rotate, grayscale, CLAHE, Gaussian smoothing [23], Laplacian-based sharpening [1], [24], and Linear Gain (Brightness boost).
8. Proposed_V2: Retinex-driven enhancement integrated with lightweight post-processing to approach the objective quality of RetinexSSR_Pctl while preserving embedded feasibility [9], [10].

2.7 Runtime and Quality Metrics

We present the following metrics by which we evaluated the different image enhancement methods:

1. Runtime: average ms/frame and FPS.
2. Entropy: Shannon entropy as a compact proxy for information content [25].
3. Edge strength: mean gradient magnitude (Sobel operator implementation as commonly described in classical imaging texts [1]).
4. Sharpness proxy: variance of Laplacian, commonly used in autofocus and sharpness estimation [26].
5. RMS contrast: intensity standard deviation, consistent with contrast interpretation in complex images [27].
6. Mean intensity: used to detect near-black runs due to auto-exposure/auto-gain drift.

Each method ran for a fixed time window (N = 20 s) and excluded an initial warm-up interval to reduce bias from exposure stabilization.

3. Results

3.1 Software Benchmarking

In Table I, we report both runtime and image-quality statistics computed per frame and averaged across four scenes. Runtime is summarized by milliseconds per frame and frames per second (FPS). Visual-information content is quantified using Shannon entropy (higher indicates a richer intensity dis- tribution). Structural detail is captured by mean edge strength (average gradient magnitude) and the variance of the Laplacian (LapVar), which increases when high-frequency components and fine boundaries are preserved. Global contrast is mea- sured using RMS contrast, while mean intensity (MeanInt) is included as a guard metric to flag near-black or saturated runs caused by auto-exposure/auto-gain drift; the number of processed frames contextualizes each average.

Overall, Table I highlights a clear trade-off between en- hancement strength and real-time feasibility on the Jetson Orin NX. RawGray is fastest (1192.78 FPS) but exhibits the weak- est visibility-related metrics (entropy 2.792, edge 3.73, RMS 9.84, mean intensity 7.08), confirming that raw NIR stream does not guarantee high night-vision quality. CLAHE provides a strong baseline improvement with minimal overhead (568.13 FPS), substantially increasing entropy (4.506) and contrast (RMS 15.89), while Bilateral+CLAHE and NLM+CLAHE further target noise at the cost of speed [2], [4], [7]. Most notably, NLM+CLAHE drops to 4.27 FPS despite similar entropy/edge levels to the other CLAHE-based variants [8]. RetinexSSR produces a large structural gain (edge 31.14, LapVar 6090.6) and raises mean intensity (107.19), but its runtime (23.32 FPS) limits interactive operation [9], [10]. The percentile variant pushes objective scores even higher (entropy 7.195, edge 96.53, RMS 42.39) yet runs at only 12.63 FPS. Proposed delivers the best balance for embedded deployment: high frame rate (269.36 FPS, 3.738 ms/frame) while improving all quality metrics over CLAHE (entropy 4.658, edge 19.36, LapVar 1155.7, RMS 19.81) with a moderate mean intensity (22.06), indicating strong detail recovery without excessive global brightening. ProposedV2 achieves the highest objective enhancement overall (entropy 7.443, RMS 50.03, LapVar 73331.7) but falls to 75.34 FPS, suggesting it is best suited for scenarios where quality is prioritized over maximum frame rate.

3.2 Qualitative Evaluation

Figure 4 provides a comparison of the output frames produced by each enhancement pipeline under the same conditions. While the objective metrics in Table I quantify information content, contrast, and structural sharpness, the visual results highlight practical perceptual differences such as noise amplification, haloing/over-brightening, and the continuity of scene edges. In particular, the figure illustrates how stronger enhancement methods reveal previously hidden structures, but may also introduce artifacts, whereas the proposed pipeline aims to recover detail while maintaining natural brightness and suppressing excessive noise.

Table 1

Mean software benchmark across four distances (100-250 cm) at 640× 480 on Jetson Orin NX. Lower is better for ms/frame. Higher is better for FPS, entropy, edge strength, LapVar, RMS contrast, and mean intensity

Method	ms/fra-me	FPS	En-tropy	Edge	LapVar	RMS	Mean Int	Fra-mes
RawGray	0.839	1192.78	2.792	3.73	197.2	9.84	7.08	897.2
CLAHE	1.761	568.13	4.506	10.7	581.9	15.89	17.65	877.7
Bilateral+CLAHE	11.432	87.56	4.544	5.72	208.7	16.29	17.79	618.2
NLM+CLAHE	234.141	4.27	4.333	3.93	199.3	15.21	16.7	71.75
RetinexSSR	42.928	23.32	5.703	31.14	6090.6	15.05	107.19	257.2
RetinexSSR-Pctl	79.222	12.63	7.195	96.53	65481.4	42.39	133.88	157.0
Proposed	3.738	269.36	4.658	19.36	1155.7	19.81	22.06	633.5
Proposed (V2)	13.274	75.34	7.443	89.27	73331.7	50.03	124.27	436.5

Figure 4

Visual comparison of the evaluated image enhancement pipelines

To further validate the contrast improvements objectively, histogram distributions were analyzed across the pipelines, as illustrated in Fig. 5. The raw grayscale frames consistently exhibit a narrow, concentrated pixel distribution, indicative of poor illumination and constrained dynamic range. Enhancement pipelines such as CLAHE, Retinex, and the Proposed methods actively stretch this distribution across the full 0–255 intensity spectrum. Notably, the Proposed version 2 (Proposed v2) method achieves a smoother and more evenly distributed histogram than standard CLAHE. This flattened distribution mathematically demonstrates that the proposed approach better utilizes the available dynamic range, mitigating the severe intensity spikes that typically correspond to noise amplification in under-exposed regions.

To extract the structural boundaries of the images, the widely adopted Canny edge detector was utilized [28], presented in Fig. 5. While spatial filtering techniques like Bilateral and NLM smoothing inherently reduce the edge strength metric by blurring fine textures, the RetinexSSR and Proposed algorithms significantly increase it. Visual analysis applying the Canny edge detector corroborates these mathematical findings; the edge maps extracted from the Proposed and Proposed V2 pipelines exhibit more continuous, pronounced, and well-defined structural boundaries compared to both the raw and CLAHE-only outputs. This confirms that, despite the computational overhead required for the more complex pipelines, the proposed methodologies successfully extract hidden structural details that are otherwise lost in low-light conditions.

A practical limitation observed during repeated runs is that auto-exposure/auto-gain drift can cause near-black frames, producing misleading metrics if not detected. Mean intensity was therefore included as a guard metric to identify invalid runs and improve repeatability.

Figure 5
Comparison of histograms of different methods

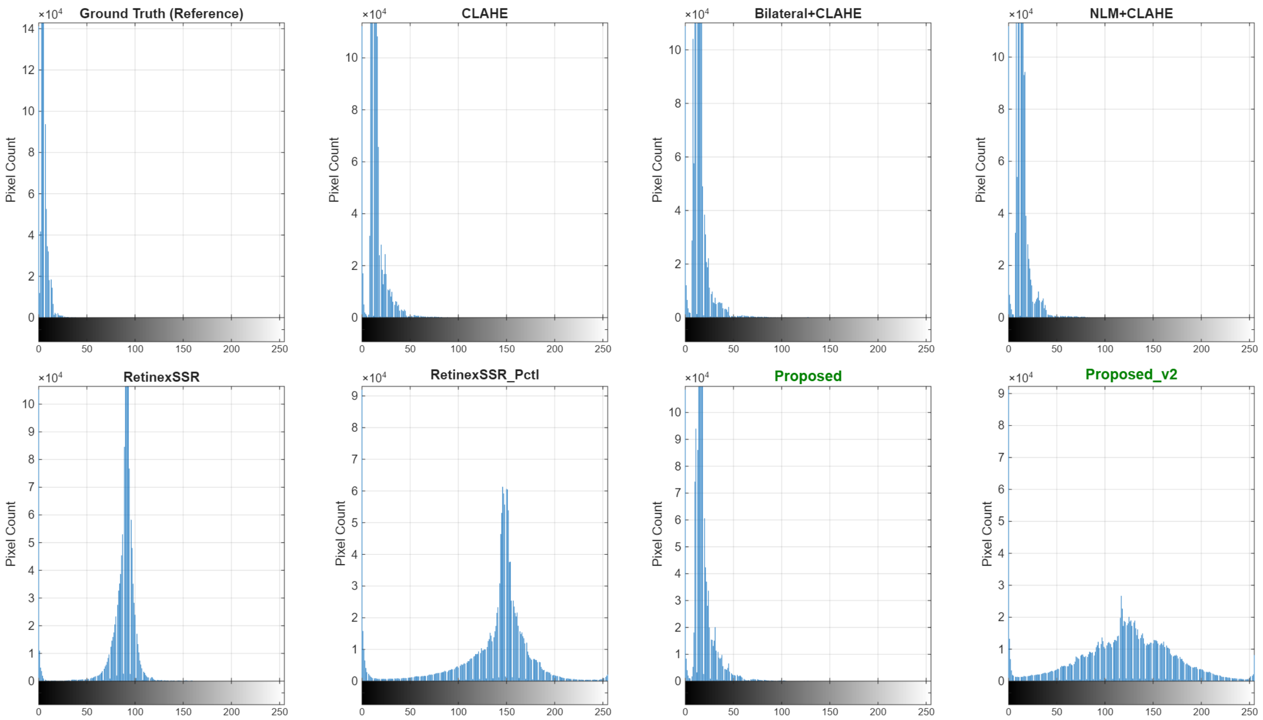

3.3 Hardware Benchmarking

To complement software benchmarking across image enhancement pipelines, we provide a qualitative visual comparison of the raw imagery captured by the tested hardware Figure 6 compares target visibility and apparent contrast under complete darkness across sensing modalities and illumination requirements, including the effect of increasing distance from the point of observation.

The thermal camera provided the clearest visibility of the target under complete darkness and required minimal tuning, demonstrating the inherent advantage of LWIR thermal sensing for night vision [14]. However, it is substantially more expensive, heavier, and less energy efficient than a consumer NIR camera, and frame acquisition required additional integration effort.

The Kinect v1 provides IR capability but required significantly stronger illumination to achieve a comparably clear intensity image. Depth sensing can reveal structure in low-light scenarios, but we excluded depth outputs to keep comparisons focused on intensity-based night-vision imagery [15].

Event-based sensing offers extremely low latency and high dynamic range [17], [18], but static objects may produce few events under constant illumination. By engineering flickering IR illumination (5 ms period), we achieved strong visibility of static targets. Nevertheless, without temporal modulation and poorer spatial resolution, the proposed NIR frame-based cam- era remains more straightforward for static-scene observation. Overall, the proposed low-cost NIR camera and lightweight enhancement provide a practical balance among cost, deployability, energy consumption, and real-time usability

Figure 6
Comparison of edge maps of different methods

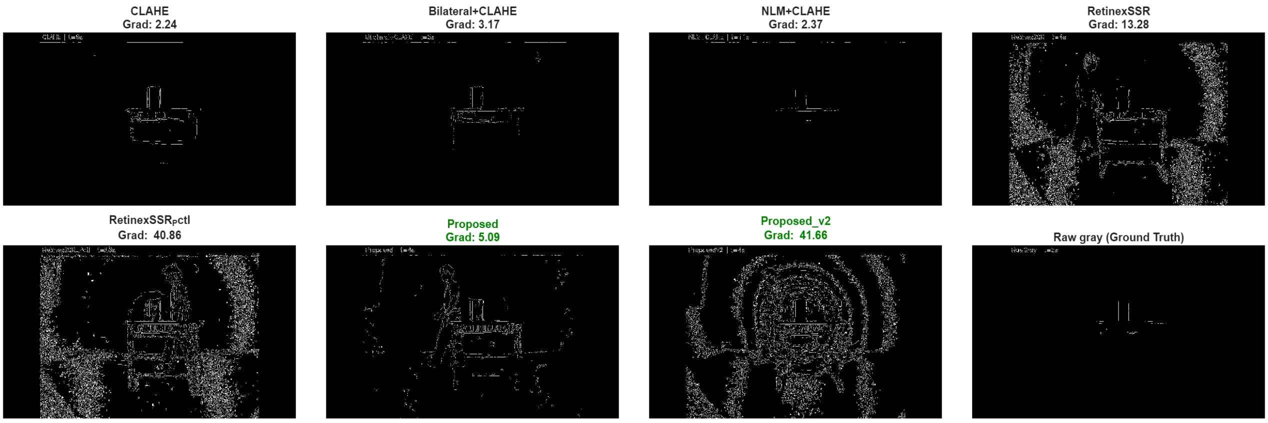

3.4 Real-Time Performance Evaluation

The system demonstrated stable operation in real time. Experiments confirmed:

1) Software processing does not result in a significant loss of frame rates.

2) The main bottleneck is data transmission over the network, not the complexity of the algorithms.

3) As the broadcast quality deteriorates, latency decreases.

4) A drop in stability was observed under Wi-Fi interference.

Therefore, the software pipeline has proven its suitability, and optimization is more likely to be required on the data transmission side than on the processing side.

3.5 Summary of Experimental Findings

Our experimental validation yields four primary conclusions regarding the feasibility of low-cost night vision:

• Spectral Sensitivity: The mechanical removal of the IR-cut filter is the foundational enabler. Without this hardware modification, the software pipeline receives insufficient photon data to recover a usable signal.

• Pipeline Synergy: The specific sequence of Grayscale → CLAHE → Denoise → Sharpen proved superior to global enhancements. Each step successfully mitigates the artifacts introduced by the previous one (e.g., Denoising correcting CLAHE-induced grain).

• Latency Bottleneck: The software pipeline, running on the Jetson platform with V4L2 optimization, introduces negligible latency. The primary bottleneck for real-time operation remains the network bandwidth required to stream the MJPEG feed to the HoloLens.

• Operational Viability: The system successfully allows for navigation in near-zero light conditions, provided that the active IR emitter is engaged to establish a minimum Signal-to-Noise Ratio for the contrast enhancement algorithms.

4. Discussion

The results of this development phase confirm that a low-cost webcam can be successfully repurposed as a night-vision imaging device when combined with a targeted infrared modification and an efficient real-time enhancement pipeline. The 850 nm IR-pass filter effectively removed visible-light interference and extended the sensor's spectral sensitivity into the near-infrared range.

The primary contribution of this work lies in the specific software pipeline developed to process raw IR-dominant frames under severe low-light conditions. In particular, the CLAHE step improved local contrast, while the denoise-then-sharpen sequence preserved edges without amplifying high-frequency noise, and the final linear gain provided a consistent brightness increase across the scene.

A key insight from our evaluation is the necessity of a "Denoise-then-Sharpen" approach. Applying sharpening directly to the noisy low-light input consistently amplified sensor noise, whereas denoising first and then restoring edges produced clearer contours and more stable visual structure, highlighting the trade-off between detail recovery and noise suppression.

Despite these successes, limitations remain. The system is heavily reliant on active infrared illumination; without a dedicated emitter, image quality degrades rapidly and usable range is reduced. In addition, overall performance is constrained by the camera sensor's inherent noise and dynamic range, and by practical bandwidth limits when streaming at higher resolutions and frame rates.

The acquired image was projected onto the Augment Reality Headset (Figure 7).

Figure 7
Visual output of Hololens 2

5. Conclusions

This paper benchmarked low-light imaging using both sensor-level hardware and software enhancement pipelines under a controlled dark-room protocol on embedded hardware. We intentionally avoided AI/ML models to prioritize lightweight real-time operation. Results show that RetinexSSR Pctl and the Retinex-integrated ProposedV2 can yield strong objective quality metrics, but are substantially slower than the proposed CLAHE-based pipeline. The proposed CLAHE-based pipeline provides the best balance of real-time FPS and image clarity under our constraints and remains suitable for streaming and mixed-reality visualization. Future work will focus on integrating Retinex-style illumination normalization into the real-time pipeline while reduc- ing computational cost (e.g., approximations, downsampling strategies, and robust normalization) so that Retinex-level quality can be approached at higher FPS. At the system level, we will improve mixed-reality usability by rendering the enhanced video as a spatially stable element in HoloLens 2 (world-locked/anchored visualization) [22].

Acknowledgement
In collaboration with Tactile Lab and ARMS Lab.

Funding
This work was supported by the Science Committee of the Ministry of Science and Higher Education of the Republic of Kazakhstan (Grant No. AP23485994)

Conflicts of Interest
All authors have read and agreed to the published version of the manuscript

Author Contributions
Conceptualization, Z.A.; Methodology, Z.A.; Software, Z.A.; Validation, Z.A.; Formal Analysis, Z.A.; Investigation, Z.A.; Resources, I.U.; Data Curation, Z.A.; Writing – Original Draft Preparation, Z.A.; Writing – Review & Editing, I.T., A.Y., Z.R. and A.B.; Visualization, Z.A.; Supervision, Z.K.; Project Administration, Z.A.; Funding Acquisition, Z.K.

References

1. R. C. Gonzalez and R. E. Woods, Digital Image Processing, 4th ed. New York, NY, USA: Pearson, 2020.
2. P. Kamboj and V. Rani, "A brief review of image denoising techniques," Vis. Comput. Ind., Biomed., Art, vol. 2, no. 8, 2019.
3. S. M. Pizer et al., "Adaptive histogram equalization and its variations," Comput. Vis. Graph. Image Process., vol. 39, no. 3, pp. 355–368, 1987.
4. K. Zuiderveld, "Contrast limited adaptive histogram equalization," in Graphics Gems IV. San Diego, CA, USA: Academic Press, 1994, pp. 474–485.
5. Y. Li, J. Lu, J. Wang, Z. Miao, and W. Xu, "Night Vision Image Contrast Enhancement Base on Adaptive Dynamic Histogram," in Proc. 4th Int. Conf. on Digital Manufacturing & Automation (ICDMA), 2013, pp. 823– 828, doi: 10.1109/ICDMA.2013.195.
6. P. Perona and J. Malik, "Scale-space and edge detection using anisotropic diffusion," IEEE Trans. Pattern Anal. Mach. Intell., vol. 12, no. 7, pp. 629–639, 1990
7. C. Tomasi and R. Manduchi, "Bilateral filtering for gray and color images," in Proc. IEEE Int. Conf. Comput. Vis. (ICCV), 1998, pp. 839– 846.

8. A. Buades, B. Coll, and J.-M. Morel, "A non-local algorithm for image denoising," in Proc. IEEE Conf. Comput. Vis. Pattern Recognit. (CVPR), 2005, pp. 60–65.

9. E. H. Land and J. J. McCann, "Lightness and retinex theory," J. Opt. Soc. Am., vol. 61, no. 1, pp. 1–11, 1971.

10. D. J. Jobson, Z. Rahman, and G. A. Woodell, "Properties and perfor- mance of a center/surround retinex," IEEE Trans. Image Process., vol. 6, no. 3, pp. 451–462, 1997.

11. X. Guo, Y. Li, and H. Ling, "LIME: Low-light image enhancement via illumination map estimation," IEEE Trans. Image Process., vol. 26, no. 2, pp. 982–993, 2017.

12. C. Wei, W. Wang, W. Yang, and J. Liu, "Deep retinex decomposition for low-light enhancement," in Proc. Brit. Mach. Vis. Conf. (BMVC), 2018.

13. C. Guo, C. Li, J. Guo, C. C. Loy, J. Hou, S. Kwong, and R. Cong, "Zero- reference deep curve estimation for low-light image enhancement," in Proc. IEEE/CVF Conf. Comput. Vis. Pattern Recognit. (CVPR), 2020, pp. 1780–1789.

14. Teledyne FLIR, "FLIR T540 professional thermal camera," 2026. [On- line]. Available: https://www.flir.com/products/t540/

15. Z. Zhang, "Microsoft Kinect sensor and its effect," IEEE MultiMedia, vol. 19, no. 2, pp. 4–12, 2012.

16. Prophesee, "EVK4-HD (Metavision evaluation kit) documentation," 2023. [Online]. Available: https://docs.prophesee.ai/stable/hw/evk/evk4.html

17. P. Lichtsteiner, C. Posch, and T. Delbr¨uck, "A 128×128 120 dB 15 μs latency asynchronous temporal contrast vision sensor," IEEE J. Solid- State Circuits, vol. 43, no. 2, pp. 566–576, 2008.

18. G. Gallego et al., "Event-based vision: A survey," IEEE Trans. Pattern Anal. Mach. Intell., vol. 44, no. 1, pp. 154–180, 2022.

19. "Low-Cost IR Night Vision System – Source Code," GitHub repository, 2025. [Online]. Available: https://github.com/YevgeniyDev/lowcost_nightvision_camera.git

20. NVIDIA, "Jetson Orin NX series data sheet," 2022. [Online]. Available: https://developer.nvidia.com/downloads/ jetson-orin-nx-series-data-sheet

21. G. Bradski, "The OpenCV library," Dr. Dobb's Journal of Software Tools, 2000.

22. Microsoft, "HoloLens 2 hardware," 2023. [Online]. Available: https://learn.microsoft.com/en-us/hololens/ hololens2-hardware

23. A. P. Witkin, "Scale-space filtering," in Proc. Int. Joint Conf. Artif. Intell. (IJCAI), 1983, pp. 1019–1022.

24. D. Marr and E. Hildreth, "Theory of edge detection," Proc. Royal Soc. London B, vol. 207, no. 1167, pp. 187–217, 1980.

25. C. E. Shannon, "A mathematical theory of communication," Bell Syst. Tech. J., vol. 27, pp. 379–423 and 623–656, 1948.

26. J. L. Pech-Pacheco, G. Crist´obal, J. Chamorro-Mart´ınez, and J. Fern´andez-Valdivia, "Diatom autofocusing in brightfield microscopy: a comparative study," in Proc. Int. Conf. Pattern Recognit. (ICPR), 2000, pp. 3318–3321.

27. E. Peli, "Contrast in complex images," J. Opt. Soc. Am. A, vol. 7, no. 10, pp. 2032–2040, 1990.

28. J. Canny, "A computational approach to edge detection," IEEE Trans. Pattern Anal. Mach. Intell., vol. 8, no. 6, pp. 679–698, 1986.

Information about the authors:

Zaki Al-Farabi – is an undergraduate student at Nazarbayev University (ORCID iD: 0009-0001-6300-4119).

Ilyas Umurbekov – holds a BS degree in Robotics from Nazarbayev University (ORCID iD: 0009-0003-1147-3196).

Iliyas Tursynbek – holds a PhD degree from Nazarbayev University (ORCID iD: 0000-0003-3753-9969).

Adilet Yesbayev – PhD, is a research assistant at Tactile Robotics Lab (ORCID iD: 0000-0002-7572-034X).

Zhanibek Rysbek – PhD, is a research assistant at Tactile Robotics Lab (ORCID iD: 0009-0003-2169-5139).

Almaskhan Baimyshev – PhD, is a research assistant at Tactile Robotics Lab (ORCID iD: 0000-0002-8494-3676).

Zhanat Kappassov – is an Associate Professor at Nazarbayev University and has over 15 years of experience in robotics, tactile sensing, artificial intelligence, and machine learning. His research interests include robotics, computer vision, and deep learning applications. He is a senior member of the Institute of Electrical and Electronics Engineers (IEEE). Dr. Kappassov has received numerous awards, including the Best PhD Thesis Award in France in 2017 and the Kazakhstani National Award for young scientists, the Kunaev Award, in 2025 (e-mail: zhkappassov@nu.edu.kz. ORCID iD: 0000-0003-3262-3993).

Submission received: 14 January, 2026
Revised: 16 March, 2026
Accepted: 16 March, 2026